Variation of Structural and Hyperfine Parameters of $(Fe_{0.70}Al_{0.30})_{1-x}Nb_x$, with x= 0, 0.05, 0.10 and 0.20 System

R R Rodríguez[1], G A Pérez Alcázar[2,3], H Colorado[2] and L E Zamora[2,3]

[1] Departamento de Ciencias Naturales, Universidad Autónoma de Occidente, Colombia
[2] Physics Department, Universidad del Valle, A.A. 25360, Cali, Colombia.
[3] Centro de Excelencia en Nuevos Materiales, Universidad del Valle, A.A. 25360, Cali, Colombia

E-mail: rrodriguez@uao.edu.co

Abstract. $Fe_{0.70}Al_{0.30}$ alloy is a bcc and ferromagnetic phase, being the Al atoms magnetic dilutor. In this work, we study the effect of the Nb on the structural and hyperfine behavior of the $Fe_{0.70}Al_{0.30}$ alloy when atoms of Nb substitute atoms of Fe or Al. The nanostructured system of $(Fe_{0.70}Al_{0.30})_{1-x}Nb_x$ (x = 0, 0.05, 0.10, 0.20, at. %) was obtained by alloying Fe, Al and Nb powders in a planetary ball mill during 12 h, 24 h and 36 h, and a ball mass to powder mass relation of 10:1. The magnetic and hyperfine properties of the samples were studied by X-ray diffraction (XRD) and Mössbauer Spectrometry (MS) at room temperature, respectively. The X-ray diffraction patterns for x=0 showed the bcc-α FeAl structure and its lattice parameter is approximately constant with milling times (~ 2.91 Å). For x=0.05, 0.10 and 0.20 the patterns showed the coexistence of the α-FeAl, $Nb(Fe,Al)_2$ structural phases with an amorphous component. The Mössbauer spectra of x=0 samples were fitted using hyperfine magnetic field distributions (HMFDs), and the obtained mean hyperfine fields (MHF) were 23.4, 24.2, and 24.3 T for 12, 24, and 36 h of milling time, respectively, which correspond to the α-FeAl structure. The spectra of the samples with x=0.05 and 0.10 were fitted using a model with two components, the first one is a HMFD attributed to the bcc-FeAlNb structure and the second with two doublets attributed to the $Nb(Fe,Al)_2$ structure. When atomic percentage of Nb increases up to 20 at. % the ferromagnetic behavior is diluted due to substitution of Fe-atoms by Nb and Al atoms in the bcc-FeAlNb structure. The magnetic behavior becomes paramagnetic at x=0.20, the spectra were fitted with three doublets, one of them related with bcc-FeAlNb structure and the others to the $Nb(Fe,Al)_2$ structural phase. The alloying of Nb to the $Fe_{0.70}Al_{0.30}$ system destroyed the magnetism due the substitution of Fe by Nb atoms and generates an amorphization into the system.

1. Introduction

Mechanical Alloying technique, originally developed to produce oxide-dispersion strengthened nickel and iron base superalloys for applications in the aerospace industry [1], has a unique capability of producing thermodynamically disfavored reactions and destabilizing equilibrium systems [2]. In fact, the large diversity of metastable systems that can be produced by MA, including amorphous alloys, supersaturated solid solutions or metastable intermetallic, makes this technique to be present in many

research fields [1-5]. Generally, high energetic milling of alloys leads to the formation of a nanocrystalline structure and, for some compositions, to amorphization [1,6].

Fe−Al alloys with strengthening intermetallic phases such as Laves phases have been identified as promising candidates for structural applications at high temperatures [7–9]. The addition of transition elements results in the precipitation of Laves phase and improves the creep resistance, in which Nb is one of the most important alloying elements [10–13]. F. Stein et al. [14] studied the as-cast microstructures of a series of ternary Fe–Al–Nb alloys, they presented a reaction scheme including the solid-state reactions and the projection of the liquids surface of the ternary system

In current work, the evolution of the properties of the $(Fe_{0.70}Al_{0.30})_{1-x}Nb_x$ (x = 0, 0.05, 0.10, 0.20, at. %) alloy obtained by mechanical alloying as a function of Nb concentration and milling times is presented. The structural and microstructural properties were obtained by X-ray diffraction (XRD) while some magnetic ones were followed by Mossbauer Spectrometry at 300 K.

2. Experimental method

Milled samples were obtained from pure element powders (iron 99.9 %, Al 99.9 % and Nb 99%), using a high energy planetary ball mill "pulverisette 5" during 12, 24, and 36 hours. The milling speed was 280 rpm and the process was carried out using a sequence of 60 minutes milling and 30 minutes resting, with a ball to powder ratio of 10:1. The elemental powders were weighted in the desired stoichiometric relation and mixed in a small flask, then transferred into the vials, under argon atmosphere.

The X-Ray diffraction (XRD) measurements were performed using a high-resolution X'Pert-MRD PANalytical diffractometer, with Co radiation, and a Fe filter. The 2θ range was from 20 to 90 degrees in steps of 0.02 degrees. All the XRD measurements were conducted at RT. The pattern refinements were realized by the Rietveld method using the General Structure Analysis System (GSAS) program [15] and the lanthanum hexaboride (LaB_6) as the calibration sample. ^{57}Fe Mössbauer experiments were performed at room temperature in transmission geometry using a conventional spectrometer with a constant acceleration mode and ^{57}Co source diffused into a rhodium matrix. The analysis of the Mössbauer spectra was done using the Mosfit program (J. Teillet, F. Varret, Unpublished Mosfit Program University of Maine) and the values of isomer shift were referred to α-Fe at 300 K.

3. Results and discussion

3.1. X-Ray Diffraction

Figure 1 presents the XRD patterns of the $(Fe_{0.70}Al_{0.30})_{1-x}Nb_x$ (x = 0, 0.05, 0.10, 0.20, at. % Nb) system milled for 36 hours. For all milling times of the sample $Fe_{0.30}Al_{0.70}$ the XRD patterns presents the peaks of α-Fe phase. The sample with x=0.05 presents the peaks of the α-Fe patterns and two additional peaks at low angles, corresponding to hcp-$Nb(Fe,Al)_2$ structure, it shows the coexistence of bcc-α-Fe-Al and hcp-$Nb(Fe,Al)_2$ structures. These results are in accord with previous works [17-20]. The peaks intensity of hcp-$Nb(Fe,Al)_2$ structure increases when Nb content increase. In the figure 1 a comparison of the background of all XRD patterns allows to establish that FeAlNb system presents a tendency to reach a highly disordered state with the increasing of Nb content, due either an amorphous state or a dense random packing of nanocrystallites of about a diameter of 2 nm.

The pattern refinements were realized with GSAS program [15]. We obtained the estimation of lattice parameter of bcc-α-Fe and Hcp - $Nb(Fe,Al)_2$ structures and their grain sizes. Table 1 shows the refined structural parameters of the phases, like their respective percentages and lattice parameters for the $(Fe_{0.70}Al_{0.30})_{1-x}Nb_x$ samples milled for 36 hours.

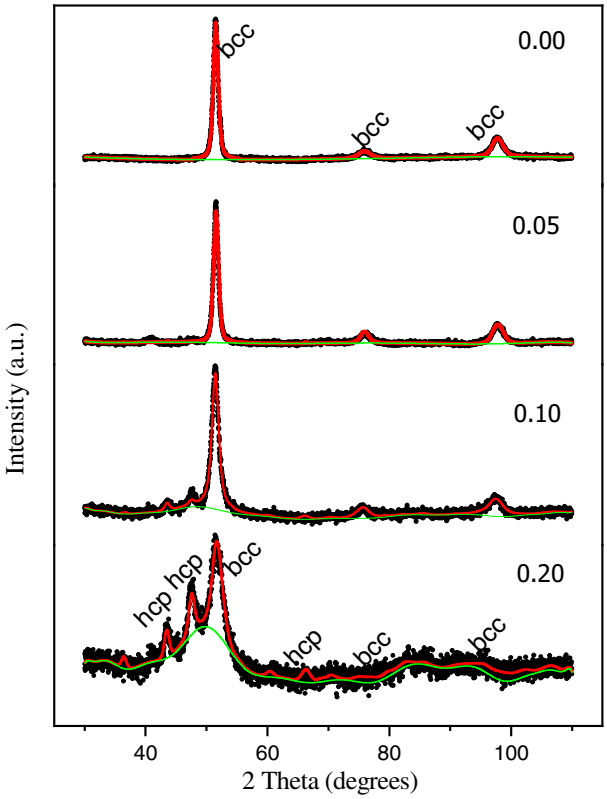

Figure 1. XRD patterns for $(Fe_{0.70}Al_{0.30})_{1-x}Nb_x$ (x = 0, 0.05, 0.10, 0.20) system milled for 36 hours.

Table 1. Structural parameters refined for the $(Fe_{0.70}Al_{0.30})_{1-x}Nb_x$ samples milled for 36 hours.

Alloy	Phase	% phase (±5)	*a* (Å) (±0.003)	*c* (Å) (±0.003)	Crystallite size (nm) (±1)
$Fe_{0.70}Al_{0.30}Nb_0$	bcc	100	2.909	--	21
$Fe_{0.675}Al_{0.285}Nb_{0.05}$	bcc	98	2.909	--	22
	hcp	2	4.837	7.982	35
$Fe_{0.63}Al_{0.27}Nb_{0.10}$	bcc	88	2.916	--	15
	hcp	12	4.867	7.660	17
$Fe_{0.56}Al_{0.24}Nb_{0.20}$	bcc	57	2.896	--	25
	hcp	43	4.843	7.870	32

The lattices parameter of bcc-structure (Figure 2) is nearly constant with Nb content up to 5 at. % for all milling times, then increases up to 10 at. %, and finally, it decreases when Nb content increases, due that Nb atoms replace Fe and Al atoms in bcc structure. The lattice parameters of hcp-$Nb(Fe,al)_2$ phase (a~4.84 Å and c~ 7.90 Å) are in agreement with those reported by others authors [20,21]. The bcc phase percentage decreases and that of the hcp increase when the Nb concentration increase. This behavior is shown in Figure 3.

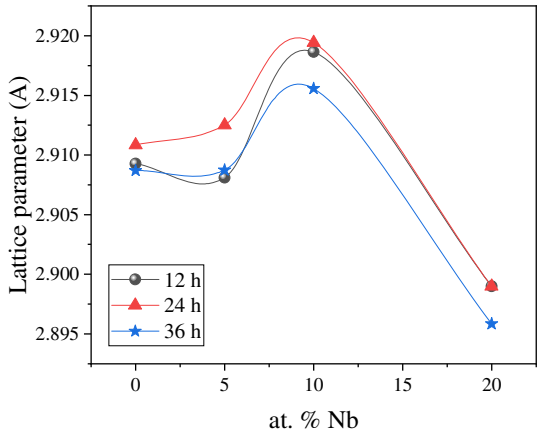

Figure 2. Lattice parameter for bcc-structure vs at. % Nb for $(Fe_{0.70}Al_{0.30})_{1-x}Nb_x$ (x = 0, 0.05, 0.10, 0.20) system.

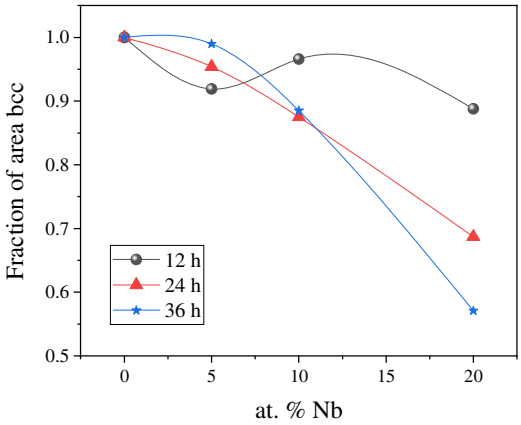

Figure 3. Percentage of bcc structural phases for $(Fe_{0.70}Al_{0.30})_{1-x}Nb_x$ (x = 0, 0.05, 0.10, 0.20, at. %) system vs Nb concentration.

3.2. Mossbauer Spectrometry

Mossbauer spectra of the $(Fe_{0.70}Al_{0.30})_{1-x}Nb_x$ (x = 0,0.05, 0.10, 0.20, at. %) alloys for 12h, 24 h and 36 hours of milling were collected. Figure 4 shows the experimental Mössbauer spectra at RT, their corresponding fitting and their hyperfine magnetic field distributions (HMFDs) of the $(Fe_{70}Al_{30})_{1-x}Nb_x$ (x = 0, 5, 10, 20, at. %) alloys with 36 hours of milling.

Table 2. Hyperfine parameters derived from the fit of RT Mossbauer spectra for $(Fe_{70}Al_{30})_{1-x}Nb_x$ alloys.

Sample	Components	δ (mm/s)	Δ (mm/s)	MHF (T)	Area (%)
$Fe_{0.70}Al_{0.30}Nb_0$	HFD	0.17	-0.04	24.3	100
$Fe_{0.675}Al_{0.285}Nb_{0.05}$	HFD	0.17	0.05	24.5	98
	Doublet 1	0.19	0.50		2
$Fe_{0.63}Al_{0.27}Nb_{0.10}$	HFD	0.13	-.028	16.9	70
	Doublet 1	-0.12	0.54		30
$Fe_{0.56}Al_{0.24}Nb_{0.20}$	Doublet 1	-0.04	0.49		49
	Doublet 2	-0.17	0.50		36
	Doublet 3	0.16	0.52		15

Estimated errors are of about ±0.02 mm/s for the isomer shift, δ, the quadrupole splitting, Δ, and of about ±2%, for the relative area, A.

The $Fe_{0.70}Al_{0.30}Nb_0$ to 12, 24 y 36 hours of milling spectrum exhibits a broad sextet, so it required a hyperfine magnetic field distribution (HMFD) to be fitted, showing the ferromagnetic and disordered character of the samples. The mean magnetic field for these alloys was of 22.4 T for 12 h milling and increases to 24.3 T for 36 h of milling, when the alloy is consolidated. These results are in accord with previous reports for the $Fe_{0.70}Al_{0.30}$ alloy [16]. For 5 and 10 at. % Nb the spectrums were fitted with the previous HMFD and a doublet. The first one was related to the α-Fe-Al structure and the second one to the $(Fe,Al)_2Nb$ phase according to XRD results. For 5 at. % Nb the MHF shows a small increase and for 10 at. % Nb the MHF presents a big decrease. It can be noted that the spectral area of the doublet increases while the hyperfine magnetic fields go to small values showing that when the Nb atoms diffuse inside the α-Fe-Al matrix diluting in this way the ferromagnetic character of the alloy. For 20 % at. Nb the spectra show a quadrupolar structure with a broad and asymmetric doublet, which was fitted with three doublets, showing that the ferromagnetic character of the sample disappears, and the sample behaves as paramagnetic. The obtained hyperfine parameters for the best fits at 36 hours milling time

are listed in Table 2. For the other milling times the behavior was like that of 36 h alloy. According with its isomer shift the doublet 1 can be associated to the α-Fe-Al with big quantity of Nb which induce the paramagnetic behavior and the doublet 2 and 3 are related with the $(Fe,Al)_2Nb$ structure and the amorphous component respectively. The hyperfine parameters are light bigger than those reported for $Fe_{0.70}Nb_{0.30}$ (IS = -0.18 mm/s and QS = 0.44 mm/s [18]). The small difference in the quadrupolar splitting is attributed to the presence of Al atoms in the hexagonal structure of $(Fe,Al)_2Nb$, this presence increase the lattice parameter and the anisotropy.

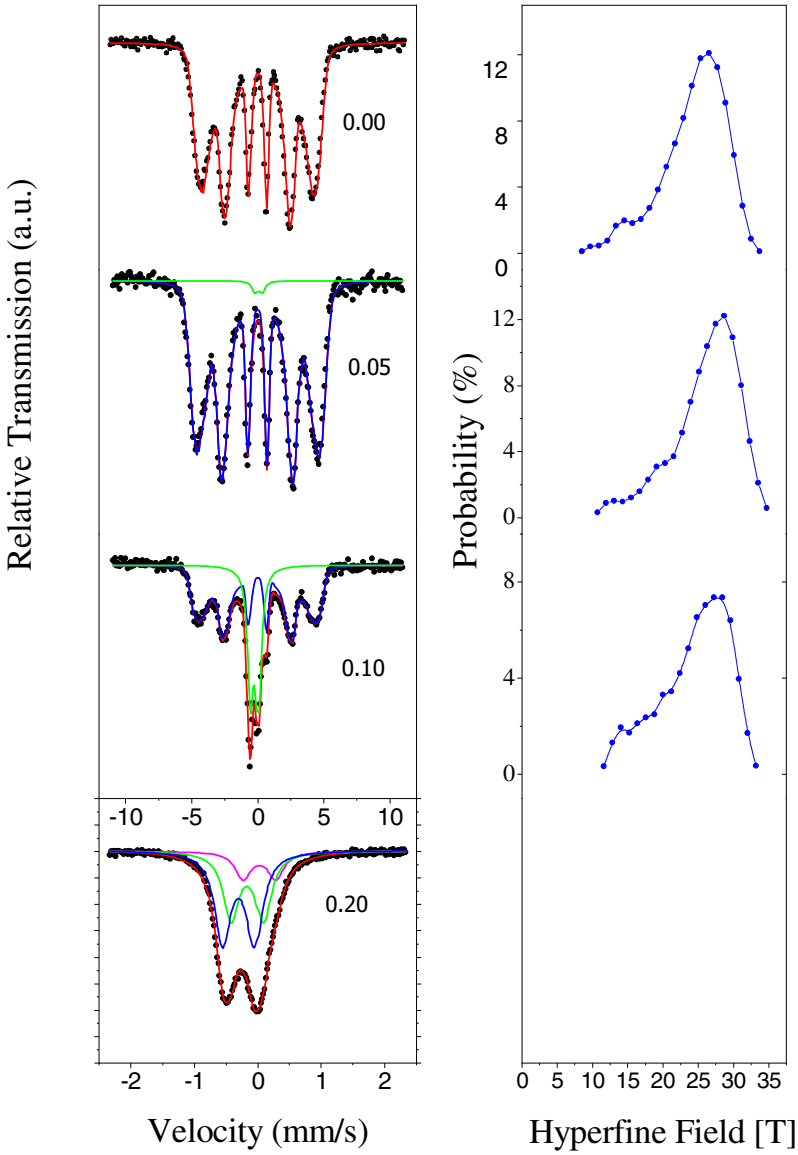

Figure 4. Mössbauer spectra at 300 K for $(Fe_{0.70}Al_{0.30})_{1-x}Nb_x$ with (X=0, 0.05, 0.10, 0.20) alloys milled for 36 hours (left) and their corresponding hyperfine fields distribution (right).

Figure 5 shows the behavior of the Mean Hyperfine Field (MHF) as a function of the Nb content. It can be appreciated that the MHF decreases with the Nb concentration until the paramagnetic behavior was obtained at 20 at. % Nb. This result is in accord with the decrease of the spectral fraction area of the HMFD and the increase of the doublet spectral area, as can be noted in Figure 6.

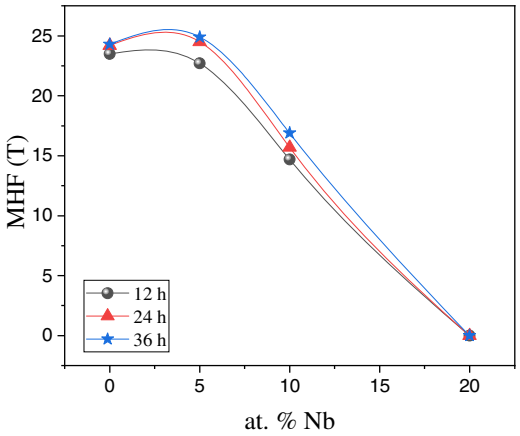

Figure 5. Mean hyperfine field vs concentration of Nb for $(Fe_{70}Al_{30})_{1-x}Nb_x$ alloys milled.

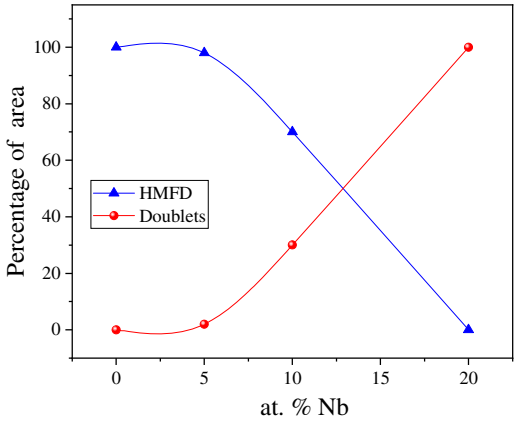

Figure. 6. Percentage of spectral area as a function of the concentration of Nb for the components used in the fit of experimental spectra of figure 1.

4. Conclusions

In this work was carried out a structural and hyperfine study of $(Fe_{70}Al_{30})_{1-x}Nb_x$ alloy system obtained by mechanical alloying. It was determined that the alloy has two structural phases, the α-FeAl, $Nb(Fe,Al)_2$ and an amorphous component. Both, increasing milling time and Nb content give rise to an increasing degree of disorder with a tendency to amorphization. Mössbauer spectrometry shows that the ferromagnetism of the alloy is affected by the diffusion of Niobium atoms in the α-FeAl structure as well as the increase in the atomic disorder of this structure until the alloy behaves as a paramagnetic.

5. Acknowledgements

This work was supported by the Universidad del Valle (Research Project C.I. 71181) and Universidad Autónoma de Occidente.

References

[1] C. Suryanarayana, 2001, Progress in Material Science. **46** 1–184.
[2] Pappas D., 2011, Journal of Vacuum Science & Technology A **29**, 020801.
[3] E.J. Lavernia, T.S. Srivatsan, 2010, The rapid solidification processing of materials: science, principles, technology, advances, and applications, J. Mater. Sci. **45** 287–325.
[4] J.S. Benjamin, T.E. Volin, 1974, The mechanism of mechanical alloying, Metallurgical Transactions, **5**, 1929–1934.
[5] J.S. Blazquez, J.J. Ipus, S. Lozano-Perez, A. Conde, 2013 Metastable soft magnetic materials produced by mechanical alloying: analysis using an equivalent time approach, JOM **65**, 870–882.
[6] A.F. Manchón-Gordón, J.J. Ipus, J.S. Blázquez, C.F. Conde, A. Conde, 2018, , Journal of Non-Crystalline Solids **494** 78–85.
[7] G. Sauthoff, 1995, Intermetallics VCH, Weinheim, Germany.

[8] L. Machon, G. Sauthoff, 1996, Intermetallics, Deformation behaviour of Al-containing Cl4 Laves phase alloys, **4**, 469–481.
[9] G. Sauthoff, 2000, Intermetallics, Multiphase intermetallic alloys for structural applications, **8**, 1101–1109.
[10] D.G. Morris, M.A. Munoz-Morris, L.M. Requejo, C. Baudin, 2006, Strengthening at high temperatures by precipitates in Fe-Al-Nb alloys, Intermetallics, 14, 1204–1207.
[11] D.G. Morris, L.M. Requejo, M.A. Munoz-Morris, 2006, Age hardening in some Fe–Al–Nb alloys, Scr. Mater. **54**, 393–397.
[12] S. Milenkovic, M. Palm, 2008, Intermetallics **16**, 1212–1218.
[13] D.G. Morris, M.A. Munoz-Morris, C. Baudin, 2004, The high-temperature strength of some Fe3Al alloys, Acta Mater. 52, 2827–2836.
[14] F. Stein,C. He, O. Prymak, S. Voß, I. Wossack, 2015, Phase equilibria in the Fe-Al-Nb system: Solidification behaviour, liquidus surface and isothermal sections, Intermetallics **59**, 43-58.
[15] A. C. Larson & R. B. Von Dreele, 2004, General Structure Analysis System (GSAS), Los Alamos National Laboratory Report LAUR 86-748.
[16] M. M. Rico, Ligia E. Zamora, G.A. Perez Alcázar, J.M. Gonzales and A. Hernando JR, 2000, Magnetic and structural study of mechanically alloyed $Fe_{0.7-X}Mn_XA_{0.30}$, Phys. Stat. sol. (b) **220**, 445.
[17] J.S. Blázquez, J.J. Ipus, C.F. Conde, A. Conde, 2012, Comparison of equivalent ball milling processes on $Fe_{70}Zr_{30}$ and $Fe_{70}Nb_{30}$, Journal of Alloys and Compounds **536S**, S9– S12.
[18] A.F. Manchón-Gordón, J.J. Ipus, J.S. Blázquez∗, C.F. Conde, A. Conde, 2018, Evolution of Fe environments and phase composition during mechanical amorphization of $Fe_{70}Zr_{30}$ and $Fe_{70}Nb_{30}$ alloys, Journal of Non-Crystalline Solids **494**, 78–85.
[19] Y. Ruan, Q.Q. Gu, P. Lü, H.P.Wang, B.Wei 2016, Rapid eutectic growth and applied performances of Fe-Al-Nb alloy solidified under electromagnetic levitation condition. Materials and Design. **112**, 239-245.
[20] D.G. Morris*, L.M. Requejo, M.A. Muñoz-Morris, 2005, A study of precipitation in DO3 ordered Fe–Al–Nb alloy, Intermetallics **13**, 862–871
[21] G.Y. Vélez, G. A. Pérez Alcázar, Ligia E. Zamora, J. A. Tabares, 2014, Structural and Magnetic Study of the Fe_2Nb Alloy Obtained by Mechanical Alloying and Sintering, J Supercond Nov Magn, **27**, 1279-1283.